Mediterranean Archaeology and Archaeometry
Vol. 20, No 2, (2020), pp. 143-158
Open Access. Online & Print.

www.maajournal.com

DOI: 10.5281/zenodo.3819601

GIS-BASED COMPARATIVE ARCHAEOLOGICAL PREDICTIVE MODELS: A FIRST APPLICATION TO IRON AGE SITES IN THE BEKAA (LEBANON)

Georges Abou Diwan

Department of Arts and Archaeology, Faculty of Letters and Human Sciences, Branch 2, Fanar, Lebanese University, Lebanon
(georges.aboudiwan@ul.edu.lb)

Received: 22/04/2020
Accepted: 01/06/2020

ABSTRACT

This study tests the use of Frequency Ratio (FR), Statistical Index (Wi), and Binary Logistic Regression (BLR) methods for establishing predictive maps for Iron Age sites in the Bekaa (Lebanon). As such it stands as the first attempt to use archaeological predictive modelling on a national level. The models were generated using an archaeological database consisting of 42 Iron Age I and 30 Iron Age II sites located in the Bekaa valley in Lebanon and six geo-environmental factors: distance to rivers, distance to cropland, slope, aspect, elevation, and terrain texture. The accuracy and predictive capacity of these models were tested using Kvamme's Gain value. The results indicate that the FR method is more reliable in locating areas of archaeological potential than Wi and BLR. The analysis of the FR- and Wi-based models shows that distance to rivers, terrain texture, and elevation provide the most significant classes affecting settlement incidence. On the other hand, in the BLR, distance to crops and distance to rivers are the most statistically significant explanatory variables for identifying areas with high archaeological probability. The archaeological predictive maps produced in this study form a valuable tool for cultural heritage management and any future archaeological investigation of the Bekaa region.

KEYWORDS: Archaeological Predictive Modelling, GIS, Frequency Ratio, Statistical Index, Binary Logistic Regression, Kvamme's Gain, Iron Age, Bekaa

1. INTRODUCTION

The present paper provides a Geographic Information System (GIS) comparative study for archaeological predictive modelling (APM) in the Bekaa valley (Lebanon) using Frequency Ratio (FR), Statistical Index (Wi), and Binary Logistic Regression (BLR). This study aims to locate the potential area in the Bekaa hosting Iron Age I and Iron II sites. The choice of this period for modelling is mainly related to its importance as a historical pivot between the settlement trends of the Bronze Age period and the emergence of new trends in the Hellenistic and Roman periods (Marfoe, 1998). The archaeological evidence related to this period in Lebanon and the Bekaa more specifically remains relatively thin (Marfoe, 1998). However, Marfoe (1995) emphasizes the archaeological potential of this region by estimating the potential existence of 300 additional sites in the Bekaa. Predictive modelling is an efficient tool in archaeological resource management (Balla et al, 2014a). It aims at investigating the archaeological potential of a specified region and establishing efficient mitigation strategies for the purpose of minimizing or avoiding the impact of anthropogenic factors. Another purpose lies in identifying the factors that influence the process of settlement selection (Eftimoski, Ross, & Sobotkova, 2017; Van Leusen et al., 2005). The present case study highlights furthermore the importance of APM given the increasingly negative impact generated by various factors such as agricultural expansion, fertilizer extraction, warfare, and urban development (Savage & Remple, 2013). The Bekaa area was subjected to numerous archaeological surveys during the past decades (Bonatz, Ali, & Jauss, 2002; Fischer-Genz & Ehrig, 2005; Hachmann, 1989; Marfoe, 1978, 1995, 1998). Most of the conducted surveys have followed conventional methods based on field walking techniques, visible sites on the 1:20,000 scale topographic maps and indications provided by the locals (Newson, 2016). While the latter approach is more fitting for small area survey, it is deemed unsuitable and time consuming for large scale mapping particularly in remote areas with limited accessibility. The use of geospatial technologies in an archaeological context has been gaining some interest during recent years in Lebanon (Abou Diwan, 2018; Abou Diwan & Doumit, 2016; Abou Diwan & Doumit, 2017; Safadi, 2013; Savage & Remple, 2013). However, the practice of APM is still largely lacking on a national level and is relatively scarce on a regional level (Al-Muheisen & Al-Shorman, 2004; Wachtel, Zidon, Garti, & Shelach-Lavi, 2018). This practice has been widely used in North American Archaeology since the 1970s. It is mainly based on the principle that the process of habitat selection is not random and is likely related to environmental and cultural variables (Verhagen, 2007; Verhagen & Whitley, 2012; Balla et al, 2014b). Numerous critical reviews have tackled the application of APM in archaeology, depicting this approach as being environmentally deterministic, thus overlooking the impact of cultural parameters in the process of habitat selection (Wheatley & Gillings, 2002). The methodological approach used for the creation of a predictive model in the present paper, variously labelled as inductive (Kamermans & Wansleeben, 1999) correlative (Judge et al., 1988) and data-driven (Wheatley & Gillings, 2002), is based on the spatial distribution of known archaeological sites and their relation to the physical properties of the landscape (Van Leusen et al., 2005; Wheatley & Gillings, 2002).

2. STUDY AREA

The study area lies within the Bekaa valley in Lebanon. It is a narrow and high plain, stretched out between the arid slopes of the Lebanon and Anti-Lebanon mountain chains. This region is characterized by a dry and continental climate with average annual precipitation greater than 700 mm in the southern part and 200 mm towards the North. This marked fluctuation in the rainfall pattern between South and North is due to the orographic effect of the Lebanese mountain chains affecting the spatial distribution of the precipitation (Traboulsi, 2010). The climatic contrast between South and North is reflected in agriculture, creating land inequality which eventually has a substantial effect on settlement patterns (Sanlaville, 1963). Geologically the area is composed of various types of rock formations with chalks, limestone, and marl from the Late Cretaceous-Neogene; limestone conglomerates and lake deposits from the Miocene as well as sand-lake deposits from the Quaternary (Dubertret, 1955; Hawie et al., 2015). The predominant soil types are calcaric, vertic, and humo-eutric cambisol (Darwish et al., 2006). The study area was delimited using the Minimum Bounding Geometry tool in ArcGIS; it represents the rectangle of the smallest area enclosing all Iron I and Iron II settlements. It extends over an area of 1,877 Km^2 ranging in altitude between 590 m and 2,194 m. The boundaries were further buffered with a 1 km distance in order to reduce the impact of artificial edge effect (Griffith 2010). This demarcation stands as the sole convenient choice given the lack of archaeological and textual data regarding the political and administrative boundaries in the Bekaa during this period. Two areas located towards the southern limits of the study region were excluded.

First, the area covered by the artificial Qaraoun lake constructed in 1959 in the vicinity of the Qaraoun village in Southern Bekaa and second the land surface which was previously covered by wetlands in central Bekaa. The latter would have covered a substantial portion of central Bekaa prior to the vast drainage operation conducted by the Mameluk during the fifteenth century. The expansion of these wetlands was recently remodelled by Abou Diwan and Doumit (2016). According to the authors, the surface area of these wetlands covered an estimated 126 km². The accuracy of their established model is further corroborated by the spatial configuration of Iron Age settlements and their absence within the modelled area (Figure 1).

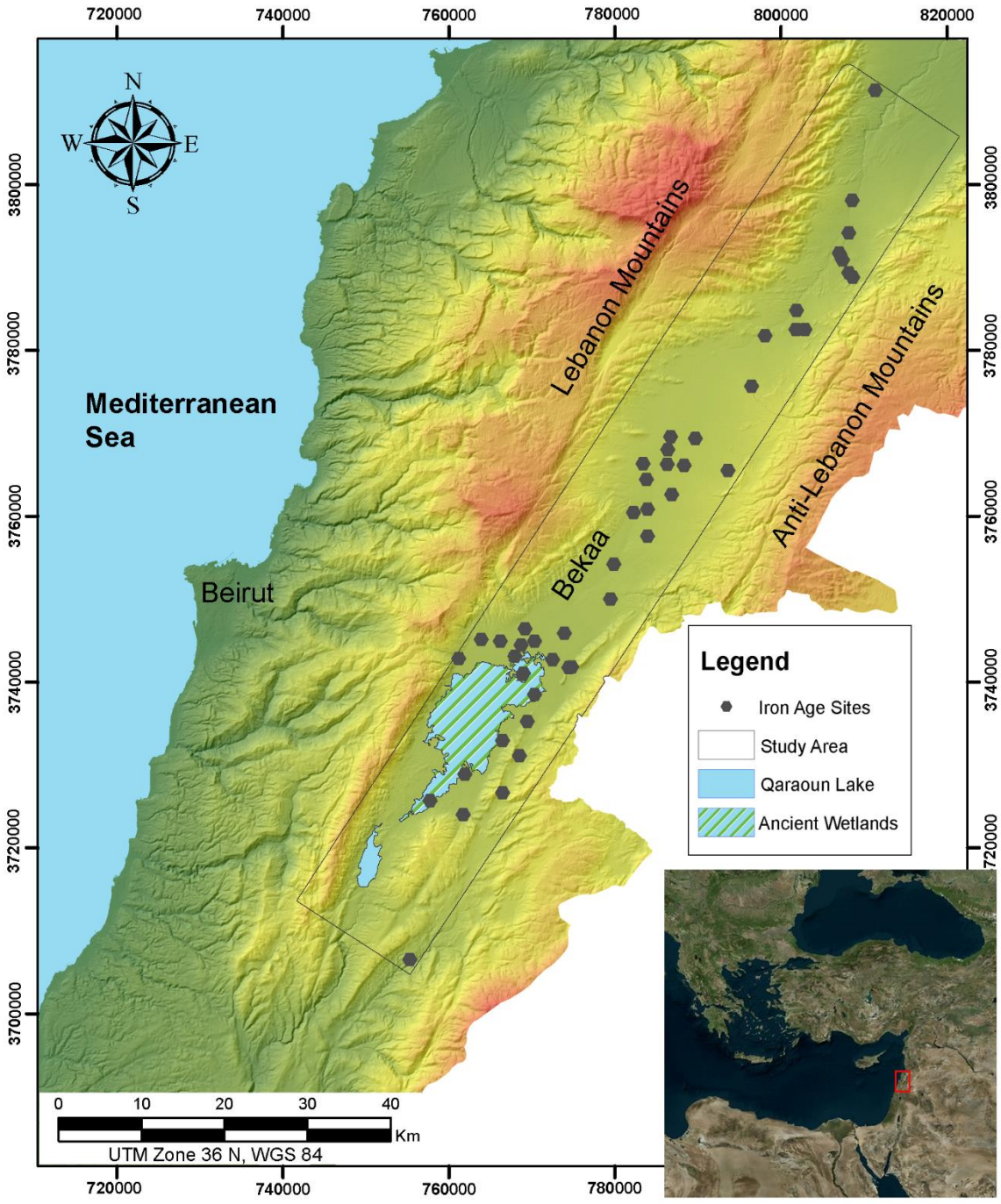

Figure 1. Geographic location of the study showing Iron Age (I-II) sites in the Bekaa (Modern Lebanon)

3. MATERIAL AND METHODS

3.1. Archaeological Data

The study began with the preparation of the archaeological database of the study area. It was initially based on the exhaustive archaeological research conducted by Marfoe between 1972 and 1974 (Marfoe, 1978, 1995). In his survey, the author recorded 401 archaeological sites ranging within a time frame from the Paleolithic to the Persian periods. The area of investigation was roughly delimited by the 1,500 m contour line with a more systematic coverage of the plain (except for water channels and wetlands) than foothills (Marfoe 1995). In his study, Marfoe undertook an analysis of archaeological site distribution according to predefined environments. The author identified four major geographical units or environments representing altitudinal zonation: valley bottom, valley border, valley sides, and mountains. Within each unit, different micro-environments were defined. The author provides a detailed description for each of these environments highlighting its main characteristics in terms of soil richness, water availability, and agricultural suitability. The distribution of Iron Age sites according to these microenvironments shows a marked preference for flood plains in both Iron Age I and II settlements with respectively 26.92% and 26.83%, whereas the geographical breakdown of sites per environment shows that 63.46% of Iron Age I and 60.97% of Iron Age II sites are located in the valley border environments (Table 1). Yet, the author does not provide a thorough explanation of the classification process used in defining these areas. This fact, along with the lack of geographical coordinates in the enclosed micro-environment map, has prevented us from integrating this study in the modelling process. Marfoe (1995, 1998) provides the size as well as the location of 52 Iron Age I and 43 Iron Age II sites in the Bekaa, based on the Lambert Levantine Grid Coordinates. However, we have chosen to incorporate 42 Iron Age I and 30 Iron Age II sites in this study. The remaining sites were discarded, given the lack of reliable dating. More recently, Savage and Remple (2013) established an updated inventory of 82 archaeological tell sites in Lebanon, of which 37 have remains from the Iron Age Period within the framework of a satellite-based condition assessment. The authors provide more accurate data for these sites in terms of geographic coordinates and settlement size. Nevertheless, we have chosen to re-evaluate this data (coordinates and size) based on newer high-resolution imagery provided by Esri Basemap Imagery. The archaeological spatial data were then projected in the Universal Transverse Mercator (UTM), Zone 36 North coordinate system (Table 2). Iron Age III sites were not included in the study considering their relatively limited number, with only ten confirmed settlements recorded so far. The lack of reliable dating is probably the reason behind this small number (Marfoe, 1998).

Table 1. The distribution of Iron Age sites according to Microenvironments (after Marfoe 1998, p. 222, fig. 48)

Environments	Microenvironments	Iron I	Iron II
Valley Bottom	Marsh Depressions	5.77%	7.32%
	Flood Plains	26.92%	26.83%
Valley Border	Karstic Spring Oases	19.23%	19.51%
	Active Alluvial Fans	21.15%	14.63%
	Lower Colluvial-Alluvial Terraces	13.46%	19.51%
	Upper Colluvial-Alluvial Terraces	9.62%	7.32%
Valley Side	Perennial Piedmont Wadis	0.00%	0.00%
	Ephemeral/ Seasonal Piedmont Wadis	1.92%	2.44%
	Rocky Piedmont Slopes and Fossil Fans	0.00%	0.00%
Outside Surveyed Area	-	1.92%	2.44%

Table 2. List of Iron Age (I-II) settlements in the Bekaa along with their updated size and coordinates.

Site Name	Easting	Northing	Area (m²)	Marfoe 1995 no.	Iron Age I	Iron Age II
Tell az-Zaytun	755334	3706712	13970	12	X	X
Kamid El-Loz	761705	3723996	51892	50	X	
Tell el-Jisr	757725	3725696	20514	51	X	
Tell 'Ayn al-Fawqa	766449	3726734	17640	66	X	
Tell Ghazze	761921	3728985	37452	107	X	
Tell Ain Meten	768495	3731123	17640	142	X	X
Tell Bir Dakoue	766454	3732940	37310	105	X	X

Tell Ain al-Khanzira	769568	3735214	23622	140	X	
Tell Deir Zenoun I	770328	3738525	87997	170	X	X
Tell Bar Elias	768931	3740992	74733	176	X	X
Tell al-Makhada	774445	3741797	18659	182	X	
Tell Neba'a Faour I	774820	3741855	30774	183	X	
Tell Serhan	772504	3742695	19113	173	X	X
Tell Kabb Elias	761225	3742859	19967	159	X	
Tell al-Majdub	767939	3743193	15369	180	X	
Tallat Karmita	768743	3744530	9211	179	X	
Tell 'Aqaibi	770362	3744923	5010	178		X
Tell Taalabaya	766211	3744988	15092	174	X	
Tell Chtaura	763906	3745184	37365	160	X	X
Tell Delhamieh	773876	3745935	41009	177	X	X
Tell 'Ain Sofar	769434	3746112	6344	186		X
Tell Rayak	779463	3750074	41354	207	X	
Tell Ain Cherif	779858	3754241	86218	206	X	X
Tell el Ghassil	783967	3757596	34645	233	X	X
Tell Hachbai	782242	3760479	44972	231	X	X
Tell Ayn Ashmal	784008	3760810	10476	236		X
Tell Hazzine	786827	3762618	30519	232	X	X
Tell Masoud	783799	3764458	17671	237	X	X
Tell Douris I	793605	3765538	17640	249	X	
Tell Majdaloun	788402	3766153	41925	234	X	X
Tell Ain Saouda	786283	3766244	9977	240		X
Tell el-Hadeth	783381	3766369	40859	269	X	X
Tell Neba'a Litani	786368	3768033	32878	268	X	X
Tell Hawsch as-Safiya	789767	3769374	35965	292	X	
Tell Aalaq	786683	3769581	28334	270	X	X
Tell Maqne II	796443	3775721	7251	294	X	X
Tell Ain Scha't	798105	3781770	26485	309	X	X
Tell Ain Ahle	802866	3782536	8362	326	X	X
Tell Rasm el Hadeth	801798	3782569	8628	324	X	
Tell el Ayyun	801868	3784867	61812	322	X	X
Tell Labwe el Yamin	808704	3788879	43033	345		X
Tell Qasr Labwe	808144	3789373	40629	344	X	X
Haql al-Bayda	807571	3790893	1510	349	X	X
Tell Sugha	807028	3791720	17500	343	X	
Tell Haql el Gami	808203	3794205	1790	348	X	X
Mrah el-Ouassa	809348	3798531	2394	362	X	
Hermel V	811385	3811352	31375	375	X	X

3.2. Geospatial Data

Different geospatial data were acquired to develop the APM:

- Topographic and morphometric derived factors such as slope, elevation, terrain texture, and aspect were computed using a 12-meter spatial resolution ALOS Palsar (Advanced Land Observing Satellite Phased Array type L-band Synthetic Aperture Radar) Digital Elevation Model (DEM) (©JAXA/METI ALOS PALSAR L1.5 2008. Accessed through ASF DAAC, June 2018).

- The cropland surface was extracted from a 1/50,000 scale land cover map of Lebanon created by The Food and Agriculture Organization of the United Nations (FAO), in cooperation with the Ministry of Agriculture. (FAO, 1990).
- Hydrological data including perennial streams were extracted from 1/20,000 scale topographic maps of Lebanon (Direction des affaires géographiques, 1966). The expanse of the artificial Qaraoun lake was extracted from the land cover map comprising the surface covered by swamp vegetation (FAO, 1990). The expanse of the ancient Bekaa wetlands mentioned in several textual sources was extracted from a study conducted by Abou Diwan and Doumit (2016).

3.3. Selected Geo-Environmental Factors

Six geo-environmental factors (independent variables) were utilized for generating the predictive models: *proximity to water, proximity to cropland, slope, aspect, elevation, and terrain texture.*

- Proximity to water sources is considered an influential factor in the establishment of settlements (Balla et al, 2013; Balla et al, 2014; Nsanziyera, Rhinane, Oujaa, & Mubea, 2018). For this purpose, we delineated the stream network of this study area from 1/20,000 scale topographic maps (Direction des affaires géographiques, 1966). Only rivers with a permanent flow pattern were selected for the modelling process. A cost surface to traverse to rivers was then created based on the Tobler Hiking Cost Function using the Path Distance Spatial Analyst Tool in ArcGIS (Tobler, 1993). The purpose is to measure the accumulative time cost of traversing each raster cell in the study area to reach the nearest available water source (Tripcevich, 2009). This method is more realistic than Euclidean Distance since the latter does not account for topographic factors such as slope or surface roughness that might impede the movement across the landscape thus imposing more time expenditure in the present case (Heilen et al., 2013). The cost distance to rivers map indicating the time required to reach water sources was reclassified into 10 different categories using the Natural Break of Jenks. This classification process was also applied to the remaining factors. The results indicate that 41.43% of the recorded Iron Age I and 52.13% of Iron Age II sites are located within a 21-minute walking distance to perennial rivers (Figure 2a).
- The availability of arable land with high suitability for agriculture use is a crucial aspect of habitat selection (Vaughn & Crawford, 2009). For this purpose, a cost surface to traverse to cropland was computed based on the Tobler Hiking Cost Function (Tobler, 1993) using the Path Distance Spatial Analyst Tool in ArcGIS. The results indicate that 92.73% of Iron Age I sites and 86.64% of Iron Age II sites are located within less than 7 minutes away from croplands. These areas are mainly characterized by calcaric, vertic, and humo-eutric cambisol soils that are deemed highly suitable for annual and perennial crops (Darwish et al., 2006) (Figure 2b).
- Slope is one of the most regularly used geomorphometric derivatives of elevation in APM since humans have a general tendency to establish their settlements on gentle slope terrains (Danese, Masini, Biscione, & Lasaponara, 2014; Graves, 2011; Mink, Ripy, Bailey, & Grossardt, 2009). The slope map of the study area was generated using the Slope Spatial Analyst Tool in ArcGIS. The results indicate that 62.37% of Iron Age I sites and 61.97% of Iron Age II sites are located in areas with a slope angle less than 6 degrees (Figure 2c).
- Aspect stands as an influential factor in the location of archaeological sites and has been tested in APM (Heilen et al., 2013; Nsanziyera et al., 2018; Verhagen etal., 2012). Aspect regions are reclassified into 10 categories according to the aspect class as: flat (−1°), north (0°–22.5°); north (337.5°–360°), northeast (22.5°–67.5°), east (67.5°–112.5°), southeast (112.5°–157.5°), south (157.5°–202.5°), southwest (202.5°–247.5°), west (247.5°–292.5°), and northwest (292.5°–337.5°). The distribution of observed archaeological sites according to aspect indicates that 40.29% of the Iron Age I and 42.96% of Iron Age II sites are located on terrains with a south-facing aspect. This preference is likely related to the fact that the south-facing slope provides high rates of sun exposure (Heilen et al., 2013) (Figure 2d).
- Elevation above sea level (altitude) is likewise a frequently employed variable in APM (Mink et al., 2009). Results show a marked preference for lower altitudes ranging between 804 and 935 masl with a percentage of 52.88% and 54.58% respectively for Iron Age I and Iron Age II sites (Figure 2e).

- Terrain texture is referred to as ''the amount of variability in elevation within a predefined radius" (Heilen et al., 2012), indicating the degree of irregularities of the surface. This factor was computed by calculating the standard deviation in elevation within a radius of 1 km using the Focal Statistics Geoprocessing Tool in ArcGIS. The percentage results show a general preference for areas with low values of surface roughness for both Iron Age I (63.34 %) and Iron Age II sites (67.55%) (Figure 2f).

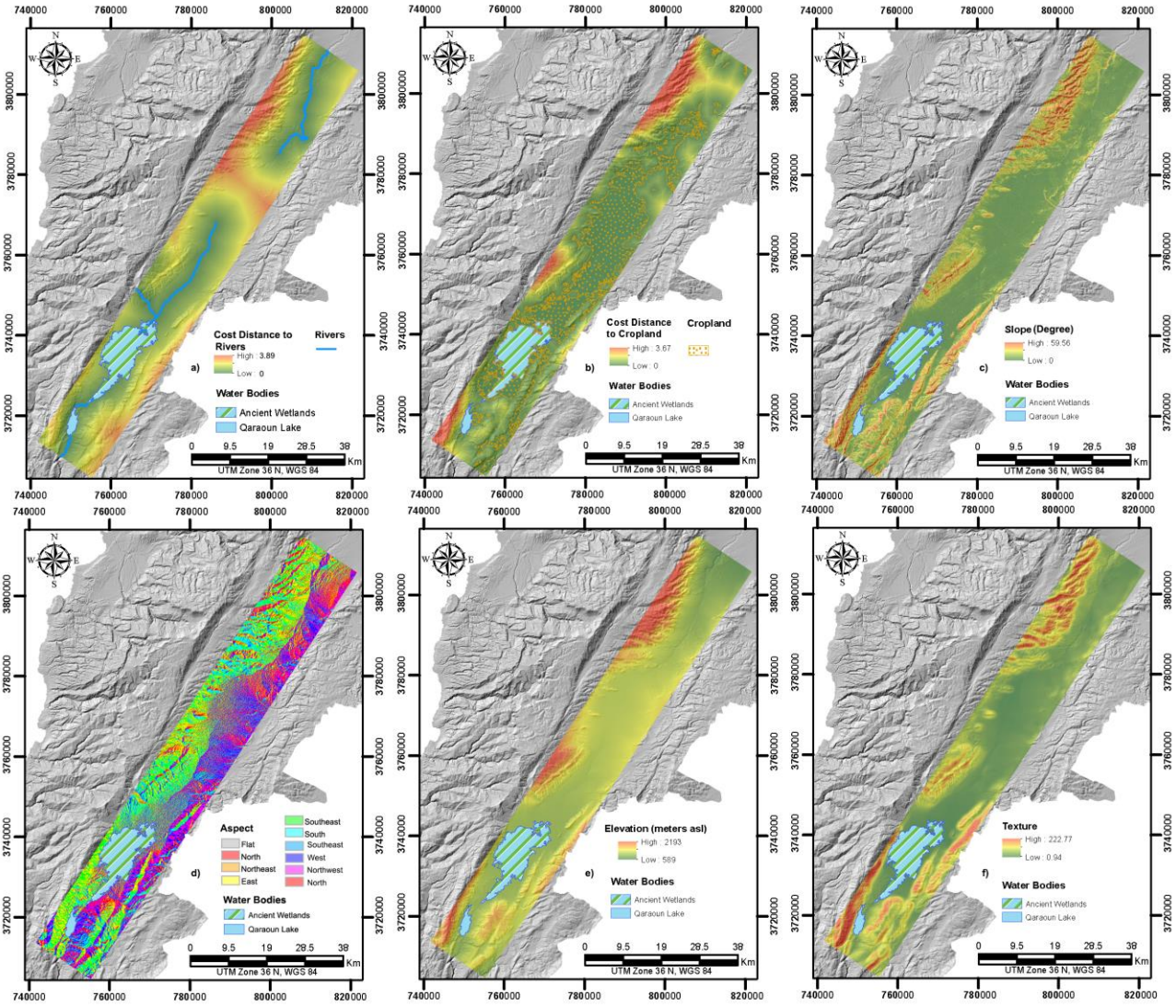

Figure 2. The selected geo-environmental factors used to compute archaeological predictive models.

3.4. Methods

3.4.1. Frequency Ratio Model (FR)

FR is one the most extensively used statistical methods in landslide susceptibility mapping (Chen et al., 2020; Lee & Talib, 2005; Yalcin et al., 2011). However, it has rarely been implemented in APM research (Aubry et al., 2012; Nicu et al., 2019). In this study, the FR examines the correlation between the distribution of archaeological sites and geo-environmental factors. The purpose is to evaluate the extent to which the selected variables in this study might have influenced the process of settlement selection (Table 3). Each factor category (class) is assigned a grade based on the ratio of the total size of the observed archaeological sites in each category to the area or spatial extent of this category. A ratio greater than 1 indicates a high correlation between a certain category and the occurrence of archaeological sites. Conversely, a ratio of less than 1 suggests that this category has less influence on archaeological site occurrence (Akgun, Dag, & Bulut, 2008). The reclassified raster classes of each factor were assigned the value of the corresponding frequency ratio values using the Lookup Spatial Analyst Tool in ArcGIS. The FR model was computed with the

Raster Calculator Spatial Analyst Tool in ArcGIS using the following equation (Lee & Talib, 2005):

$$APM = Fr_1+Fr_2+Fr_3+\ldots+Fr_n$$

where FR is the rating of each factor.

3.4.2. Statistical Index Model (Wi)

The Wi method is an extensively used model in the field of geosciences and landslide susceptibility mapping (Yalcin et al., 2011). It has not been applied to APM up to this date. It aims to show in this case a statistical relationship between the distribution of Iron Age settlements and the selected geo-environmental factors. A weight value is therefore assigned to each category (class) of these factors. This is done by computing the natural logarithm of the archaeological density in each category (class), divided by the archaeological density inside the whole factor (Table 3). Positive values are assigned to a higher than average archaeological density, while negative values indicate a lower than normal frequency (Rautela & Lakhera, 2000; Van Westen, 1997). The Wi method was computed according to the following formula:

$$\ln Wi = \ln\left(\frac{Densclas}{Densmap}\right) = \ln\left(\frac{\frac{Npix(Si)}{Npix(Ni)}}{\frac{\sum Npix(Si)}{\sum Npix(Ni)}}\right)$$

where

Wi = The weight given to a certain factor category (class)

Densclas = Archaeological density within the factor category (class)

Densmap = Archaeological density within the entire factor map

Npix (Si) = Number of pixels that contain archaeological sites in a certain factor category (class)

Npix (Ni) = Total number of pixels in a certain factor category (class)

The Wi values are assigned to the reclassified raster factor using the Lookup Spatial Analyst Tool. All six geo-environmental factors are then combined to generate the APM using the Raster Calculator Spatial Analyst Tool.

Table 3. Frequency Ratio and Statistical Index values assigned to the categories (classes) of each factor.

Factors	*Categories (classes)*	*Area % (a)*	*Sites % (b)*		*Frequency Ratio (FR) (b/a)*		*Statistical Index (Wi)*	
			Iron Age I	**Iron Age II**	**Iron Age I**	**Iron Age II**	**Iron Age I**	**Iron Age II**
Cost Distance to Rivers (Time travel in hours)	0-0.35	15.12%	41.43%	53.12%	2.74	3.51	1.01	1.26
	0.36-0.70	15.60%	26.81%	29.35%	1.72	1.88	0.54	0.63
	0.71-1.04	15.38%	17.22%	6.62%	1.12	0.43	0.11	-0.84
	1.05-1.37	13.83%	8.49%	12.04%	0.61	0.48	-0.49	-0.73
	1.38 – 1.71	12.76%	4.01%	6.66%	0.31	0.15	-1.16	0.00
	1.72 – 2.05	9.54%	0.27%	1.91%	0.03	0.00	-3.55	0.00
	2.06 – 2.38	7.60%	1.16%	0.00%	0.15	0.00	-1.88	0.00
	2.39 – 2.75	5.39%	0.60%	0.00%	0.11	0.00	-2.20	0.00
	2.76 – 3.18	2.91%	0.00%	0.00%	0.00	0.00	0.00	0.00
	3.19 – 3.89	1.88%	0.00%	0.00%	0.00	0.00	0.00	0.00
Cost Distance to Cropland (Time travel in hours)	0-0.12	46.97%	92.73%	86.64%	1.97	1.84	0.68	0.61
	0.13-0.33	17.74%	7.27%	13.36%	0.41	0.75	-0.89	-0.28
	0.34-0.59	12.31%	0.00%	0.00%	0.00	0.00	0.00	0.00
	0.6-0.88	7.54%	0.00%	0.00%	0.00	0.00	0.00	0.00
	0.89-1.21	4.91%	0.00%	0.00%	0.00	0.00	0.00	0.00
	1.22-1.57	3.04%	0.00%	0.00%	0.00	0.00	0.00	0.00
	1.58-1.95	2.70%	0.00%	0.00%	0.00	0.00	0.00	0.00
	1.96-2.34	2.24%	0.00%	0.00%	0.00	0.00	0.00	0.00
	2.35-2.84	1.45%	0.00%	0.00%	0.00	0.00	0.00	0.00
	2.85-3.68	1.09%	0.00%	0.00%	0.00	0.00	0.00	0.00
Slope (degree)	0 – 2.8	31.64%	25.15%	26.84%	0.79	0.85	-0.23	-0.16
	2.81 - 5.84	22.92%	37.22%	35.13%	1.62	1.53	0.48	0.43
	5.85 - 9.58	13.16%	30.47%	30.91%	2.32	2.35	0.84	0.85
	9.59 - 13.32	9.29%	5.83%	6.03%	0.63	0.65	-0.47	-0.43
	13.33 - 17.05	7.35%	1.16%	0.98%	0.16	0.13	-1.84	0.00
	17.06 - 20.79	5.85%	0.16%	0.12%	0.03	0.02	-3.58	0.00
	20.8 - 24.53	4.47%	0.00%	0.00%	0.00	0.00	0.00	0.00
	24.54 - 28.5	3.14%	0.00%	0.00%	0.00	0.00	0.00	0.00
	28.51 - 33.41	1.67%	0.00%	0.00%	0.00	0.00	0.00	0.00
	33.42 - 59.57	0.52%	0.00%	0.00%	0.00	0.00	0.00	0.00
	Flat (-1)	0.00%	0.00%	0.00%	0.00	0.00	0.00	0.00
	North	5.48%	4.72%	4.70%	0.86	0.86	-0.15	-0.15

	(0-22.5)							
Aspect	Northeast (22.5-67.5)	10.28%	10.14%	10.66%	0.99	1.04	-0.01	0.04
	East (67.5-112.5)	13.64%	15.60%	15.77%	1.14	1.16	0.13	0.15
	Southeast (112.5-157.5)	17.16%	16.94%	17.61%	0.99	1.03	-0.01	0.03
	South (157.5-202.5)	11.77%	9.72%	10.54%	0.83	0.90	-0.19	-0.11
	Southwest (202.5-247.5)	9.00%	13.63%	14.81%	1.51	1.65	0.41	0.50
	West (247.5-292.5)	11.48%	11.75%	10.11%	1.02	0.88	0.02	-0.13
	North West (292.5-337.5)	14.97%	10.63%	9.93%	0.71	0.66	-0.34	-0.41
	North (337.5-360)	6.23%	6.88%	5.88%	1.10	0.94	0.10	-0.06
Elevation (msl)	589 - 803	5.69%	2.64%	3.24%	0.46	0.57	-0.77	-0.56
	804 - 935	21.06%	52.88%	54.58%	2.51	2.59	0.92	0.95
	936 - 1,036	25.27%	40.21%	40.29%	1.59	1.59	0.46	0.47
	1,037 - 1,136	17.77%	4.03%	1.89%	0.23	0.11	-1.48	-2.24
	1,137 - 1,250	10.62%	0.24%	0.00%	0.02	0.00	-3.80	0.00
	1,251 - 1,375	7.30%	0.00%	0.00%	0.00	0.00	0.00	0.00
	1,376 - 1,526	4.90%	0.00%	0.00%	0.00	0.00	0.00	0.00
	1,527 - 1,696	3.35%	0.00%	0.00%	0.00	0.00	0.00	0.00
	1,697 - 1,885	2.73%	0.00%	0.00%	0.00	0.00	0.00	0.00
	1,886 - 2,193	1.32%	0.00%	0.00%	0.00	0.00	0.00	0.00
Terrain Texture	1-13	24.07%	64.34%	67.55%	2.67	2.81	0.98	1.0
	14-28	21.16%	18.53%	25.18%	0.88	1.19	-0.13	0.2
	29-45	14.58%	10.60%	3.82%	0.73	0.26	-0.32	-1.3
	46-64	12.42%	4.77%	3.10%	0.38	0.25	-0.96	-1.4
	65-82	8.63%	1.75%	0.35%	0.20	0.04	-1.60	0.0
	83-99	7.47%	0.00%	0.00%	0.00	0.00	0.00	0.0
	100-118	5.97%	0.00%	0.00%	0.00	0.00	0.00	0.0
	119-140	3.45%	0.00%	0.00%	0.00	0.00	0.00	0.0
	141-171	1.71%	0.00%	0.00%	0.00	0.00	0.00	0.0
	172-223	0.53%	0.00%	0.00%	0.00	0.00	0.00	0.0

3.4.3. Binary Logistic Regression Model (BLR)

BLR is a commonly used predictive analysis equation in APM (Holton Jr, 2014; Vaughn & Crawford, 2009; Wachtel et al., 2018; Zhu et al., 2018). It examines the relationship between a binary dependent variable which in this case is the presence or absence of archaeological sites, and a set of an independent variables (the six geo-environmental factors). The latter could be continuous, categorical, or binary and do not necessarily have a normal distribution. The logistic regression function will model the probability of occurrence of an event in a binary outcome, namely the presence or absence of archaeological sites based on the selected factors (predictors variables). The predicted probabilities are then translated using a sigmoid cost function to values constrained between 0 and 1, as explained in the equation below (Hosmer & Lemeshow, 2000):

The model is Prob (Y) $=\frac{1}{1+e^{-Z}}$

where Prob (Y) is the probability of an event occurring with a value equal to 0 denoting the absence of archaeological sites and a value equal to 1 indicating the presence of archaeological sites; Z is the linear combination, $Z = B_0 + B_1.X_1 + B_2.X_2 + \ldots + B_n.X_n$; B_0 is the intercept or the constant of the model; B_n is the slope coefficient of the regression model, and X is the value of the selected independent variable. The logistic regression was computed using the Statistical Package for the Social Sciences (SPSS). The Forward Likelihood Ratio method was chosen to define the most significant independent variables to use in modelling the predictive map with Sig. values lower than 0.05. The accuracy of the model was assessed using the Omnibus tests of model coefficients to test whether the new models, including the independent variables, are different from the base model with the intercept. The results show an enhancement in the accuracy of both Iron Age I and II models as can be seen with the high chi-squared values and sig. values less than 0.05 (Table). The Hosmer and Lemeshow test was also used to examine the goodness of fit of the model. Low Chi-squared values with larger Sig. values (closer to 1) indicate a good logistic regression model fit (Hosmer & Lemeshow, 2000) (Table 5). The pseudo-r-squared statistic Nagelkerke's R2 was also calculated to evaluate the capacity of the independent variables in

`predicting the dependent variable. A value equal to 1 indicates a perfect fit, whereas a value of zero shows no relationship (Menard, 2008). A relatively good fit is confirmed for a value greater than 0.2 (Clark & Hosking, 1986) which is the case for this study with values of 0.469 for Iron Age I and 0.578 for Iron Age II sites. Finally, the most statistically significant variables retained for establishing the predictive maps are cost distance to cropland, cost distance to rivers, and aspect. The predictive model for Iron Age I and II sites was created with the Raster Calculator Spatial Analyst Tool in ArcGIS, using the equations below. The generated predictive maps have a value ranging between 0 to 1, with 1 representing the highest likelihood of settlement incidence.

APM Iron I= 1 div (1 + (exp (- (-1.775 + (-7.409* cost distance to cropland) + (-1.330* cost distance to rivers)))))

APM Iron II= 1 div (1 + (exp (- 3.189+ (-8.321* cost distance to cropland) + (-1.595 * cost distance to rivers) + (-0.009 * aspect)))))

Table 4 Omnibus Tests of Model Coefficients

Iron Age I	Chi-square	df	Sig.
Step	15.423	1	0.000
Block	39.721	2	0.000
Model	39.721	2	0.000
Iron Age II	**Chi-square**	**df**	**Sig.**
Step	7.636	1	0.006
Block	44.183	3	0.000
Model	44.183	3	0.000

Table 5 Hosmer-Lemeshow goodness-of-fit test

Iron 1	Chi-Square	df.	Sig.
Step 1	8.559	8	0.381
Step 2	3.540	8	0.896
Iron 1I	**Chi-Square**	**df.**	**Sig.**
Step 1	10.533	8	0.230
Step 2	2.839	8	0.944
Step 3	13.323	8	0.101

4. RESULTS AND DISCUSSION

The final APMs generated using the methods above were classified into five probability classes: very low, low, moderate, high, and very high using natural breaks of Jenks (Figure 3). In terms of evaluating the precision of the computed predictive maps, defined by Verhagen (2008) as the capacity of the model to narrow down the limit of the area with the highest probability, the results show that the FR models exhibit the best results for Iron Age I sites with 16.66% of the total surface of the study. As for Iron Age II sites, the BLR model seems to outperform the other models with a percentage of 11.69 (Figure 4). In terms of assessing the accuracy of the models, defined as the ability of the highest probability area to capture most of the archaeological sites (Verhagen, 2008), the calculation was first performed based on the distribution percentage of archaeological site surfaces. The results show a better performance for the Wi method in both Iron Age I and II sites with respectively 74.53% and 74.97% of the total archaeological surface falling in the Very High Probability Class (Figure 5). The number-based distribution percentage of archaeological sites displays approximately similar results as the surface-based distribution. The highest percentages of archaeological sites are recorded using the Wi method with 71.43% for Iron Age I and 73.33% for Iron Age II settlements (Figure 6). The performance assessment of the predictive model was examined using simple Gain statistics after Kvamme and expressed using the following formula: (Kvamme, 1988).

$$G = 1- (\%PS / \%GS)$$

Where G is the gain mode, PS is the percentage of the area characterized by the highest probability of hosting archaeological sites, and GS is the percentage of observed archaeological sites within this area. Further, we have also performed the calculation based on the percentage of observed archaeological surfaces. The gain values extend from 0 to 1. A value closer to 1 indicates high accuracy in predicting archaeological sites. The calculated gain for Iron Age I models shows a better performance for the FR method with respectively a value of 0.75 and 0.70 for surface and number-based approach. As for Iron Age II models, the highest recorded K gain value using the surface-based method is registered in the FR, with 0.81. The number-based approach exhibits slightly different K gain values with the BLR model at the forefront, followed by the FR with respectively 0.82 and 0.79 (Table 6, Table 7). In any event, the overall picture which emerges from this study shows that the FR Method provides a more consistent indicator to the archaeological potential of the Bekaa during the Iron Age Periods. Although Kavmme's gain values remain one of the widely used methods for testing the validity of archaeological predictive models, major downsides have been highlighted in the scholarly literature as this test method is based on the same data used for the computation of the APM. The use of an independent random sample survey remains, according to critics, one of the best solutions for

testing the accuracy of the model (Gibbon, 2002; Verhagen, 2008).

As stated above, the selection of geo-environmental factors for computing the predictive model is based on the assumption that the natural environment played an influential role in the process of habitat selection in ancient societies. The relative impact of these variables is detected through the implemented methodological approach. The analysis of the FR and Wi methods shows that the areas located within a 21-minute walking distance to rivers have significant impact on the incidence of Iron Age sites. Regarding distance to crops, the areas located within a 7-minute walking distance are likewise highly favorable to the establishment of settlements. Slope, elevation and terrain texture respectively ranging between 5.85 – 9.58 degree, 804 – 935 m and 1-13 are the most important classes affecting archaeological sites occurrence. As for aspect, the southern direction has the most significant impact on the incidence of Iron Age sites. It can therefore be concluded that distance to rivers, terrain texture, and elevation have the most significant categories in the process of generating predictive models. The BLR method shows that distance to crops and distance to rivers are the most statistically significant explanatory variables concerning settlement selection.

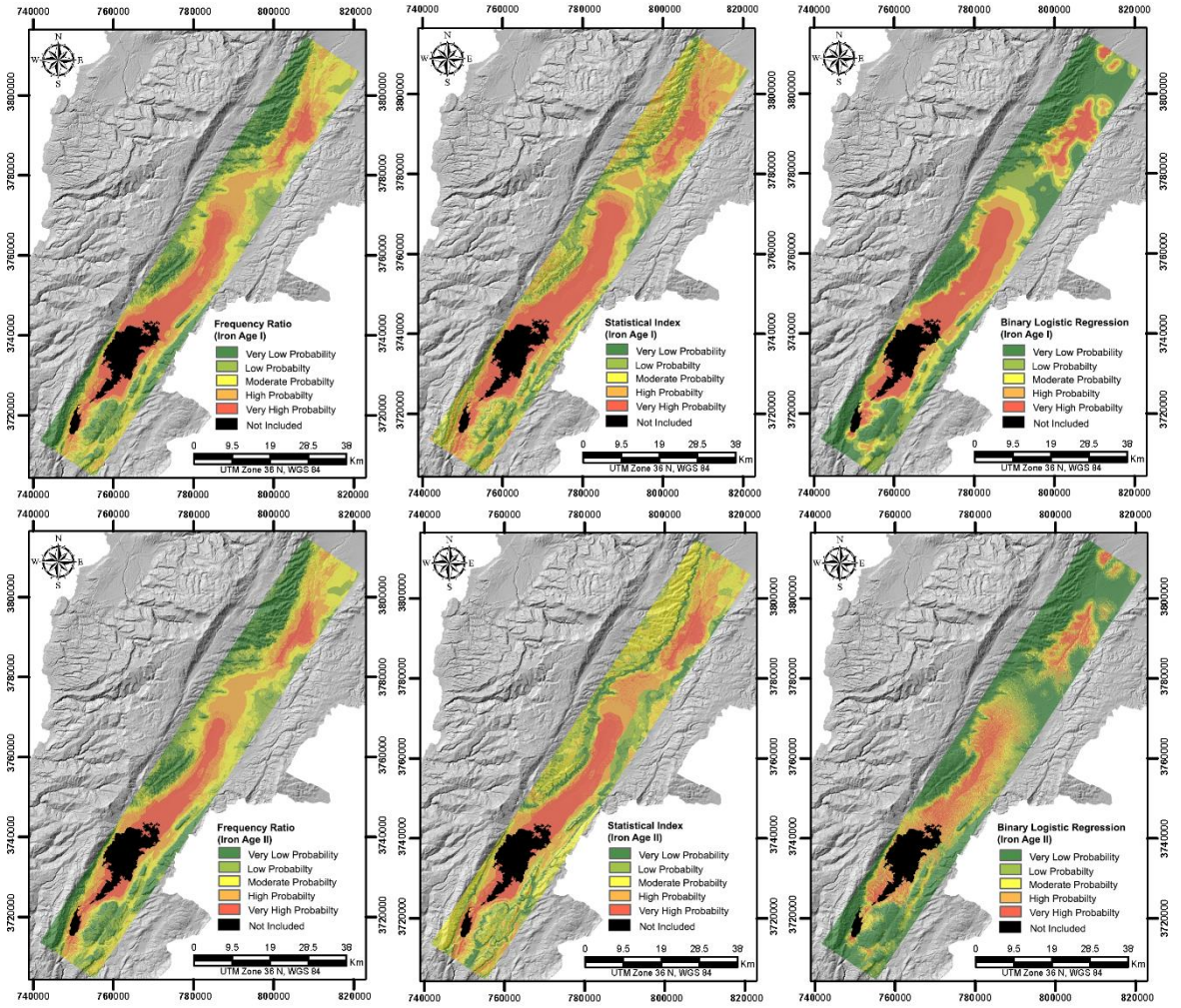

Figure 3. The archaeological predictive maps based on FR, Wi and BLR (The areas highlighted in black were not incorporated to the study)

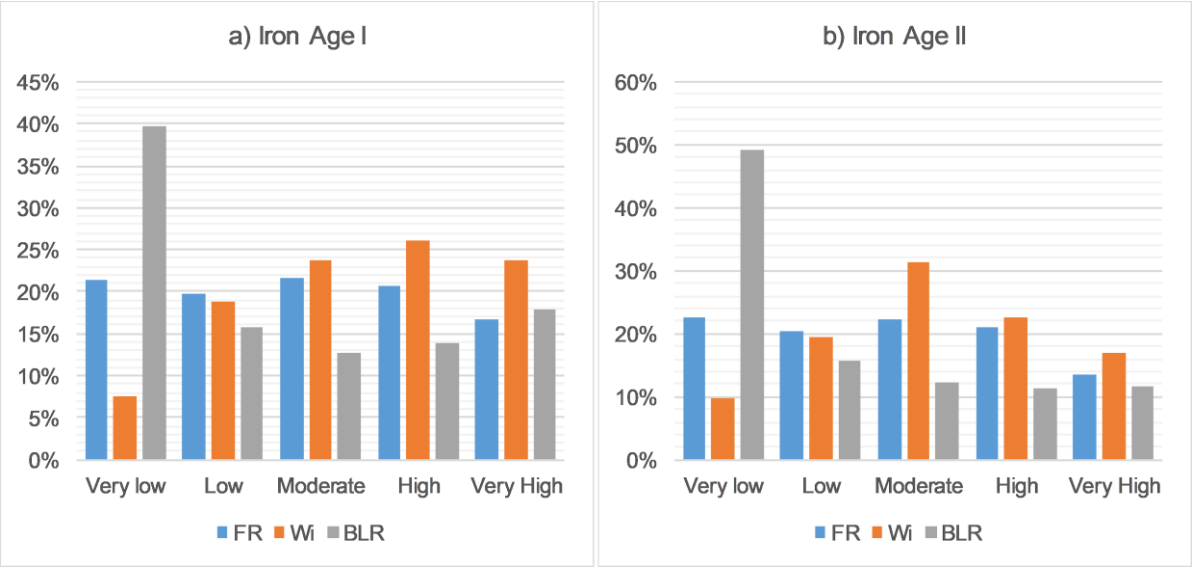

Figure 4. The surface percentage of each probability class

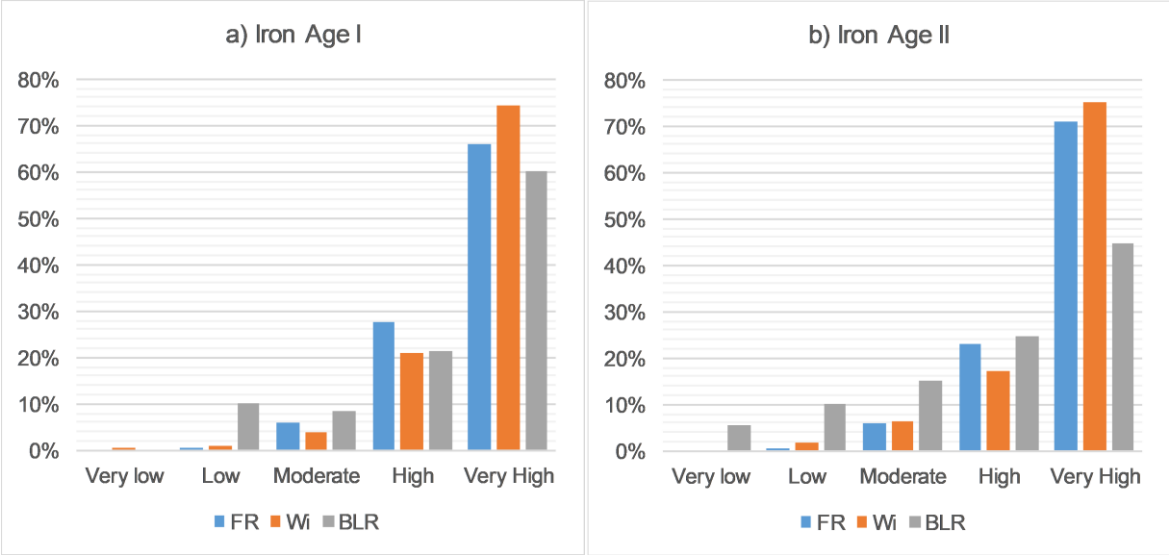

Figure 5. The archaeological surface percentage within each probability class

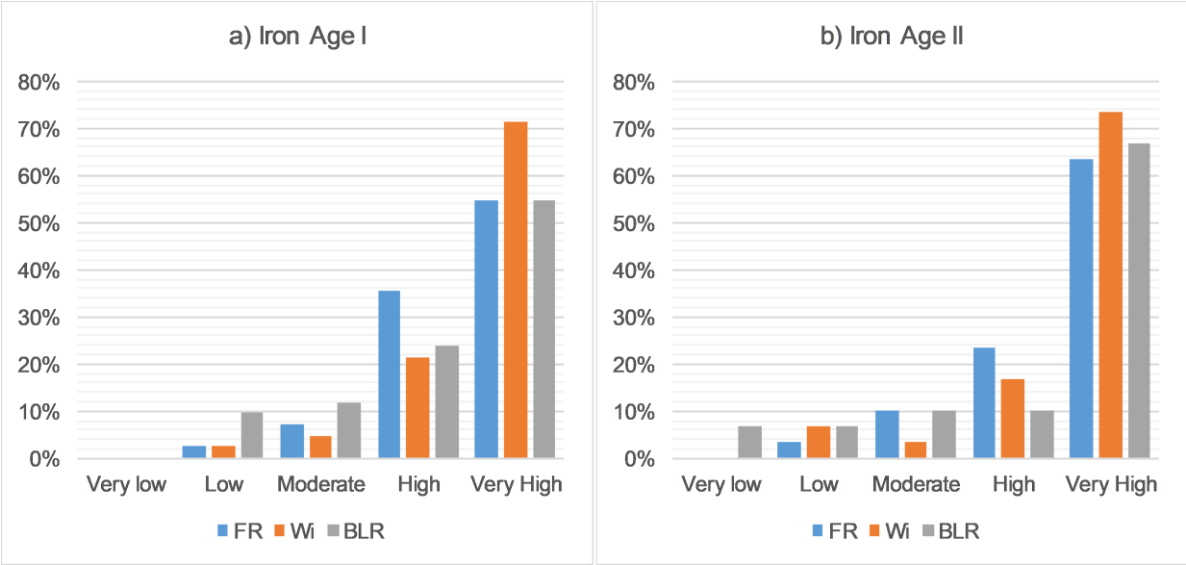

Figure 6. The archaeological sites percentage within each probability class

Table 6. Kvamme's gain values based on the percentage of the observed surface of archaeological sites

Probability	Iron I			Iron II		
	FR	SI	BLR	FR	SI	BLR
Very low	-	-149.3	-	-	-	-8.25
Low	-49.96	-23.06	-0.53	-93.66	-10.92	-0.56
Moderate	-2.60	-5.08	-0.51	-2.76	-4.04	0.19
High	0.26	-0.26	0.35	0.08	-0.31	0.54
Very High	0.75	0.68	0.70	0.81	0.77	0.74

Table 7 Kvamme's Gain values based on the percentage of the observed number of archaeological sites

Probability	Iron I			Iron II		
	FR	SI	BLR	FR	SI	BLR
Very low	-	-	-	-	-	-6.37
Low	-7.29	-6.95	-0.65	-5.13	-1.91	-1.36
Moderate	-2.02	-3.98	-0.08	-1.23	-8.41	-0.22
High	0.42	-0.22	0.42	0.10	-0.35	-0.12
Very High	0.70	0.67	0.67	0.79	0.77	0.82

5. CONCLUSION

The use of APM has not been previously employed in Lebanese archaeology. This study presented three methodological approaches for creating an APM for Iron Age (I-II) sites in the Bekaa. The applied methods are qualified as inductive. They are based on the statistical analysis of archaeological settlement location relative to geo-environmental independent variables. The FR and BLR have been implemented in previous APM studies, while the application of the Wi model is being tested for the first time in archaeology. These methods had not yet been comparatively evaluated in APM before the present study. The results show that all models have proven to be objective, yielding reliable results in terms of weight attribution and the evaluation of the impact of each factor as can be detected through Kvamme's gain values. Comparatively speaking, the FR model has generally proven to have a relatively higher prediction accuracy for Iron Age I-II sites using the surface-based approach. K gain value based on archaeological site numbers confirms the stated results for Iron Age I sites but indicates a slightly better performance of BLR for Iron Age II sites. The generated prediction maps form an efficient tool in the framework of risk assessment of the cultural heritage of the Bekaa and a platform for any future archaeological investigations in this area.

REFERENCES

Abou Diwan, G. (2018). Finding Chalcis ad Libanum: A GIS-based Approach. *Geo-Sp Mag, 7*(21), 15-32.

Abou Diwan, G., & Doumit, J. (2016). Ancient Wetlands of the Biqā: A Buffer Zone Between the Hinterlands of Sidon and Berytus in the Roman Period. *Bulletin d'Archéologie et d'Architecture Libanaises, 16*, 215-254.

Abou Diwan, G., & Doumit, J. (2017). The Berytus-Heliopolis Baalbak Road in the Roman Perod: A Least Cost Path Analysis. *Mediterranean Archaeology and Archaeometry, 17*(3), 225-241.

Akgun, A., Dag, S., & Bulut, F. (2008). Landslide susceptibility mapping for a landslide-prone area (Findikli, NE of Turkey) by likelihood-frequency ratio and weighted linear combination models. *Environmental Geology, 54*(6), 1127-1143.

Al-Muheisen, Z., & Al-Shorman, A. (2004). The archaeological site of Bediyeh: The constructed landscape. *Syria, 81*, 177-189.

Aubry, T., Luís, L., & Dimuccio, L. A. (2012). Nature vs. Culture: present-day spatial distribution and preservation of open-air rock art in the Côa and Douro River Valleys (Portugal). *Journal of Archaeological Science, 39*(4), 848-866.

Balla, A., Pavlogeorgatos, G., Tsiafaki, D., & Pavlidis, G. (2014a). Recent advances in archaeological predictive modeling for archeological research and cultural heritage management. *Mediterranean Archaeology and Archaeometry, 14* (4), 143-153.

Balla, A., Pavlogeorgatos, G., Tsiafaki, D., & Pavlidis, G. (2014b). Efficient predictive modelling for archaeological research. *Mediterranean Archaeology and Archaeometry, 14* (1), 119-129.

Balla, A., Pavlogeorgatos, G., Tsiafakis, D., & Pavlidis, G. (2013). Locating Macedonian tombs using predictive modelling. *Journal of Cultural Heritage, 14*(5), 403-410. doi:10.1016/j.culher.2012.10.011

Bonatz, D., Ali, N., & Jauss, C. (2002). Preliminary remarks on an archaeological survey in the Anti-Lebanon. *Bulletin d'Archéologie et d'Architecture Libanaises 6*, 283-307.

Chen, W., Fan, L., Li, C., & Pham, B. T. J. A. S. (2020). Spatial prediction of landslides using hybrid integration of artificial intelligence algorithms with frequency ratio and index of entropy in nanzheng county, china. *Applied Sciences*, *10*(1), 29.

Clark, W. A. V., & Hosking, P. L. (1986). *Statistical methods for geographers*. New York: John Wiley & Sons.

Danese, M., Masini, N., Biscione, M., & Lasaponara, R. (2014). Predictive modeling for preventive Archaeology: overview and case study. In *Open Geosciences* (Vol. 6, pp. 42).

Darwish, T., Khawlie, M., Daher, M., Jomaa, I., Awad, M., Masri, T., Kheir, R. (2006). *Soil Map of Lebanon 1:50000*.

Dubertret, L. (Cartographer). (1955). Carte géologique du Liban.

Eftimoski, M., Ross, S. A., & Sobotkova, A. (2017). The impact of land use and depopulation on burial mounds in the Kazanlak Valley, Bulgaria: An ordered logit predictive model. *Journal of Cultural Heritage, 23*, 1-10. doi:https://doi.org/10.1016/j.culher.2016.10.002.

FAO (Cartographer). (1990). Land cover map of Lebanon. Scale 1/50000.

Fischer-Genz, B., & Ehrig, H. (2005). First results of the archaeological survey project in the territory of ancient Heliopolis-Baalbek. *Bulletin d'Archéologie et d'Architecture Libanaises, 9*, 135-138.

Direction des affaires Géographiques du Liban, (Cartographer). (1966). Carte du Liban 1:20,000.

Gibbon, G. (2002). *Appendix A: Archaeological Predictive Modelling: An Overview*. (SHPO Reference Number 95-4098). Minnesota Department of Transportation Retrieved from http://www.mnmodel.dot.state.mn.us/chapters/app_a.htm. [10 April 2020].

Graves, D. (2011). The use of predictive modelling to target Neolithic settlement and occupation activity in mainland Scotland. *Journal of Archaeological Science, 38*(3), 633-656. doi:https://doi.org/10.1016/j.jas.2010.10.016.

Hachmann, R. (1989). Preliminary remarks on an archaeological survey in the Anti-Lebanon 1963-1981. German excavation in Lebanon. Part One. *Berytus, 37*, 5-187.

Hawie, N., Deschamps, R., Granjeon, D., Nader, F., Gorini, C., Müller, C., Baudin, F. (2015). Multi-scale constraints of sediment source to sink systems in frontier basins: a forward stratigraphic modeling case study of the Levant region. *Basin Research*, 1-28. doi:10.1111/bre.12156.

Heilen, M., Leckman, P., Byrd, A., Homburg, J., & A. Heckman, R. (2013). *Archaeological Sensitivity Modeling in Southern New Mexico: Automated Tools and Models for Planning and Management* (SRI Technical Report 11-26). Retrieved from

Heilen, M., Leckman, P. O., Byrd, A., Homburg, J. A., & Heckman, R. A. (2013). Archaeological sensitivity modeling in southern New Mexico: Automated tools and models for planning and management. *Statistical Research, Inc. Technical Report, Albuquerque, NM*, 11-26.

Holton Jr, J. T. (2014). *Predictive Model of Archaeological Sites of the Hopi Reservation of Northeastern Arizona.* (Masters), University of Redlands, Retrieved from http://inspire.redlands.edu/gis_gradproj/222

Hosmer, D. W., & Lemeshow, S. (2000). Applied logistic regression.

Judge, W. J., Sebastian, L., Altschul, J. H., Ebert, J. I., Kincaid, C. T., Kohler, T. A., Piper, J.-E. (1988). *Quantifying the present and predicting the past : theory, method, and application of archaeological predictive modeling*: U.S. Department of the Interior, Bureau of Land Management ; For sale by the Superintendent of Documents, U.S. Government Printing Office.

Kamermans, H., & Wansleeben, M. (1999). *Predictive modelling in Dutch archaeology, joining forces.* Paper presented at the New Techniques for Old Times – CAA98. Computer Applications and Quantitative Methods in Archaeology.

Kvamme, K. (1988). *Development and testing of Quantitative models.* Paper presented at the Quantifying the Present and Predicting the Past: Theory, Method and Application of Archaeological Predictive Modelling.

Lee, S., & Talib, J. A. (2005). Probabilistic landslide susceptibility and factor effect analysis. *Environmental Geology, 47*(7), 982-990.

Marfoe, L. (1978). *Between Qadesh and Kumidi: A History of Frontier Settlement and Land Use in the Biqa', Lebanon*: University of Chicago, Regenstein Library, Department of Photoduplication.

Marfoe, L. (1995). *Kāmid el-Lōz. 13, The prehistoric and early historic context of the site : catalog and commentary* (Vol. 41). Bonn: Habelt.

Marfoe, L. (1998). *Kāmid el-Lōz. 14, Settlement history of the Biqā' up to the Iron Age* (Vol. 53). Bonn: Habelt.

Menard, S. (2008). *Applied logistic regression analysis*. Thousand Oaks, Calif.: Sage.

Mink, P. B., Ripy, J., Bailey, K., & Grossardt, T. H. (2009). *Predictive Archaeological Modeling using GISBased Fuzzy Set Estimation: A Case Study in Woodford County, Kentucky*. Retrieved from Kentucky Transportation Center Faculty and Researcher Publications: https://uknowledge.uky.edu/ktc_facpub/12

Newson, P. (2016). Archaeological landscapes of the Bekaa: past results and future prospects. *Berytus, 56*, 257-280.

Nicu, I. C., Mihu-Pintilie, A., & Williamson, J. (2019). GIS-Based and Statistical Approaches in Archaeological Predictive Modelling (NE Romania). *Sustainability, 11*(21), 59-69.

Nsanziyera, A., Rhinane, H., Oujaa, A., & Mubea, K. (2018). GIS and Remote-Sensing Application in Archaeological Site Mapping in the Awsard Area (Morocco). *Geosciences, 8*(6), 207.

Nsanziyera, A. F., Lechgar, H., Fal, S., Maanan, M., Saddiqi, O., Oujaa, A., & Rhinane, H. (2018). Remote-sensing data-based Archaeological Predictive Model (APM) for archaeological site mapping in desert area, South Morocco. *Comptes Rendus Geoscience, 350*(6), 319-330.

Rautela, P., & Lakhera, R. C. (2000). Landslide risk analysis between Giri and Tons Rivers in Himachal Himalaya (India). *International Journal of Applied Earth Observation and Geoinformation, 2*(3), 153-160. doi:https://doi.org/10.1016/S0303-2434(00)85009-6.

Safadi, C. (2013). *The Beq'a Valley during the Early Bronze Age: A GIS Approach to settlement pattern*. (Master of Science in Archaeological Computing-Spatial Technologies), University of Southampton.

Sanlaville, P. (1963). Les régions agricoles du Liban. *Revue de géographie de Lyon, 38*(1), 47-90. doi:10.3406/geoca.1963.1751

Savage, S. H., & Remple, S. (2013). *Climate Change and Human Impact on Ancient and Modern Settlements: Identification and Condition Assessment of Archaeological Sites in the Northern Levant from Landsat, ASTER and CORONA Imagery*.

Tobler, W. (1993). *Three presentations on geographical analysis and modeling*, Santa Barbara, University of California.

Traboulsi, M. (2010). La pluviométrie moyenne annuelle au Liban : Interpolation et cartographie automatique. *Lebanese Science Journal,11* (2), 2010, 11-25.

Tripcevich, N. (2009). Cost Distance Analysis. Retrieved from http://mapaspects.org/node/3744. Accessed June 10, 2018.

Van Leusen, M., Deeben, J., Hallewas, D., Zoetbrood, P., Kamermans, H., & Verhagen, P. (2005). A baseline for predictive modelling in the Netherlands. In M. Van Leusen & H. Kamermans (Eds.), *Predictive modelling for archaeological heritage management: A research agenda* (pp. 25-92). Amersfoort.

Van Westen, C. J. (1997). *Statistical landslide hazard analysis*. ILWIS 2.1 for Windows application guide. ITC Publication, Enschede, 73–84.

Vaughn, S., & Crawford, T. (2009). A predictive model of archaeological potential: An example from northwestern Belize. *Applied Geography, 29*(4), 542-555. doi:10.1016/j.apgeog.2009.01.001.

Verhagen, P. (2007). *Case studies in archaeological predictive modelling* (Vol. 14): Leiden University Press

Verhagen, P. (2008). *Testing archaeological predictive models: a rough guide.* Paper presented at the CAA2007 - Layers of Perception. Proceedings of the 35th International Conference on Computer Applications and Quantitative Methods in Archaeology., Berlin, Germany, April 2–6, 2007.

Verhagen, P., Nuninger, L., Tourneux, F.-P., Bertoncello, F., & Jeneson, K. (2012). *Introducing the human factor in predictive modelling: a work in progress.* Paper presented at the Archaeology in the digital era. Papers from the 40th annual conference of computer applications and quantitative methods in archaeology (CAA), Southampton.

Verhagen, P., & Whitley, T. G. (2012). Integrating Archaeological Theory and Predictive Modeling: a Live Report from the Scene. *Journal of Archaeological Method, 19*(1), 49-100. doi:10.1007/s10816-011-9102-7

Wachtel, I., Zidon, R., Garti, S., & Shelach-Lavi, G. (2018). Predictive modeling for archaeological site locations: Comparing logistic regression and maximal entropy in north Israel and north-east China. *Journal of Archaeological Science, 92*, 28-36. doi:https://doi.org/10.1016/j.jas.2018.02.001

Wheatley, D., & Gillings, M. (2002). *Spatial technology and archaeology : the archaeological applications of GIS*. London: Taylor & Francis.

Yalcin, A., Reis, S., Aydinoglu, A. C., & Yomralioglu, T. (2011). A GIS-based comparative study of frequency ratio, analytical hierarchy process, bivariate statistics and logistics regression methods for landslide susceptibility mapping in Trabzon, NE Turkey. *Catena, 85*(3), 274-287. doi:10.1016/j.catena.2011.01.014

Zhu, X., Chen, F., & Guo, H. (2018). A Spatial Pattern Analysis of Frontier Passes in China's Northern Silk Road Region Using a Scale Optimization BLR Archaeological Predictive Model. *Heritage, 1*(1), 15-32. doi:10.3390/heritage1010002.